A LETTERS JOURNAL EXPLORING THE FRONTIERS OF PHYSICS

LETTER • OPEN ACCESS

Fluctuation-dissipation in thermoelectric sensors

To cite this article: N. A. M. Tran *et al* 2023 *EPL* **141** 26002

A Letters Journal Exploring the Frontiers of Physics

January 2023

EPL, **141** (2023) 26002
doi: 10.1209/0295-5075/acb009

www.epljournal.org

Fluctuation-dissipation in thermoelectric sensors

N. A. M. Tran[1], A. S. Dutt[2], N. B. Pulumati[2], H. Reith[2], A. Hu[1], A. Dumont[3], K. Nielsch[2], A.-M. S. Tremblay[3], G. Schierning[4], B. Reulet[3] and T. Szkopek[1(a)]

[1] *Department of Electrical and Computer Engineering, McGill University - Montréal, Québec, H3A 0E9, Canada*
[2] *Institute for Metallic Materials, IFW Dresden - 01069 Dresden, Germany*
[3] *Département de physique et Institut Quantique, Université de Sherbrooke - Sherbrooke, Québec, J1K 2R1, Canada*
[4] *Faculty of Physics, Universität Bielefeld - 33501 Bielefeld, Germany*

received 5 September 2022; accepted in final form 4 January 2023
published online 19 January 2023

Abstract – Thermoelectric materials exhibit correlated transport of charge and heat. The Johnson-Nyquist noise formula $4k_BTR$ for the spectral density of voltage fluctuations accounts for fluctuations associated solely with Ohmic dissipation. Applying the fluctuation-dissipation theorem, we generalize the Johnson-Nyquist formula for thermoelectrics, finding an enhanced voltage fluctuation spectral density $4k_BTR(1+Z_DT)$ at frequencies below a thermal cut-off frequency f_T, where Z_DT is the dimensionless thermoelectric device figure of merit. The origin of the enhancement in voltage noise is thermoelectric coupling of temperature fluctuations. We use a wideband ($f_T \sim 1\,\text{kHz}$), integrated thermoelectric micro-device to experimentally confirm our findings. Measuring the Z_DT enhanced voltage noise, we experimentally resolve temperature fluctuations with a root mean square amplitude of $0.8\,\mu\text{K}\,\text{Hz}^{-1/2}$ at a mean temperature of 295 K. We find that thermoelectric devices can be used for thermometry with sufficient resolution to measure the fundamental temperature fluctuations described by the fluctuation-dissipation theorem.

Introduction. – The fluctuation-dissipation theorem [1] relates the fluctuations in a system at thermodynamic equilibrium with the coefficient of irreversible dissipation under an externally applied bias field. In an electrical conductor, the fluctuation-dissipation theorem takes the form of the Johnson-Nyquist noise formula for voltage fluctuations $\langle V^2 \rangle = 4k_BTR\Delta f$, where k_B is Boltzmann's constant, T is absolute temperature, R is the electrical resistance, and Δf is the electrical bandwidth [2,3]. The resistance R that quantifies the irreversible dissipation of electrical conduction also determines the amplitude of voltage fluctuations at equilibrium. Owing to its generality, the fluctuation-dissipation theorem has been applied to various physical systems, including quantum optics [4].

Considering fluctuations in an electrical conductor further, fundamental excitations in condensed matter carry not only charge, but other physical quantities such as, for example, heat, spin, and pseudo-spin. The *thermoelectric* response of a conductor is a result of the correlated transport of charge and heat by fundamental excitations. In the simplest scenario, the Seebeck coefficient S is a measure of the mean entropy carried per unit charge e, and the Peltier coefficient $\Pi = TS$ is a measure of the mean thermal energy carried per unit charge e [5–7]. Correlations in the fluctuation of charge and heat transport have been considered theoretically in nanoscale systems [8–11], and the role of charge fluctuations in non-linear thermoelectric response of superconducting junctions has been investigated [12,13].

Surprisingly, the fluctuation-dissipation theorem as it applies to a thermoelectric material and the resulting correlations in fluctuation of charge current, heat current, voltage and temperature have not been investigated to date. Temperature fluctuation at equilibrium is well-known in the theory of statistical mechanics [14,15], but typically eludes measurement in condensed matter owing to the small absolute scale of temperature fluctuations, which scales inversely with heat capacity. The first experimental measurement of spontaneous temperature fluctuations was observed in a paramagnetic salt in cryogenic conditions by magnetometry [16]. Temperature fluctuations are of prime importance in various

(a) E-mail: thomas.szkopek@mcgill.ca (corresponding author)

phenomena in condensed matter as for example they limit the sensitivity of bolometers [17], generate dynamical phase transitions [18] and are at the origin of non-Gaussian fluctuations in metals [19,20]. Micro-scale and nano-scale thermoelectric thermometry is of increasing interest for scanning thermal microscopy [21], cellular-level thermometry [22–25], semiconductor circuit thermometry [26], and wearable sensors [27,28], further motivating the understanding of fluctuations in thermoelectrics.

In this paper, we apply the fluctuation-dissipation theorem to derive a generalized Johnson-Nyquist formula for thermoelectrics, revealing a modification in the spectral density of fluctuations that is dependent on the dimensionless, material thermoelectric figure of merit $zT = \Pi S/\kappa\rho$ (not to be confused with device $Z_D T$, see eq. (11)), where κ is the thermal conductivity and ρ is the electrical resistivity. Using integrated, wide-bandwidth, thermoelectric micro-devices [29] in a Λ leg-pair configuration and operated with a thermally floating terminal suitable for thermometry, we measure the spectral density of voltage fluctuations and find agreement with the generalized Johnson-Nyquist formula for thermoelectrics. In the spirit of the fluctuation-dissipation theorem, experimental impedance spectroscopy is further used to explicitly test the correspondence between irreversible transport coefficients and equilibrium fluctuations in a thermoelectric material.

Results. –

Fluctuation-dissipation analysis. We first consider fluctuations in a uniform thermoelectric material, before considering a thermoelectric device. The relationship between electric current I_e, heat current I_Q in a thermoelectric material of length L and cross-sectional area A in the presence of a time-dependent potential difference ΔV and temperature difference ΔT across the length L,

$$\begin{aligned} I_e &= L'_{11}\Delta V + L'_{12}\frac{\Delta T}{T} + C'_e\frac{\partial}{\partial t}\Delta V, \\ I_Q &= L'_{21}\Delta V + L'_{22}\frac{\Delta T}{T} + C'_Q\frac{\partial}{\partial t}\Delta T, \end{aligned} \tag{1}$$

where $L'_{ij} = (A/L)L_{ij}$ are the extensive transport coefficients, satisfying Onsager's reciprocal relation $L'_{12} = L'_{21}$. This transport model is appropriate at time scales long compared to electron-phonon scattering times, such that electrons and phonons are in local equilibrium and a single temperature profile can be used to describe temperature variation across the thermoelectric. The temperatures at opposite sides of the thermoelectric are T and $T + \Delta T$, with the temperature difference $\Delta T \ll T$ such that a linear transport model applies.

The intensive transport coefficients L_{ij} are related to electrical conductivity σ, Seebeck coefficient S, thermal conductivity κ,

$$\sigma = L_{11}, \quad S = -\frac{1}{T}\frac{L_{12}}{L_{11}}, \quad \kappa = \frac{1}{T}\frac{L_{22}L_{11} - L_{12}L_{21}}{L_{11}}. \tag{2}$$

The dynamical response of the thermoelectric depends upon the extensive heat capacity $C'_Q = \partial U/\partial \Delta T$, where U is the heat transported across the length L of the thermoelectric. For $\Delta T \ll T$, where the temperature varies linearly across the length L of the thermoelectric, the heat capacity $C'_Q = c_q AL/2$, where c_q is the volumetric specific heat and the factor of $1/2$ accounts for the mean increase in temperature of $\Delta T/2$ over the body of the thermoelectric. Electrical capacitance is given by $C'_e = \partial Q/\partial \Delta V$, where Q is the charge separation across the thermoelectric. Our analysis and subsequent experiments concern frequencies below the electrical cut-off frequency, $2\pi f_e = L'_{11}/C'_e$, and thus the displacement current $C'_e \partial\Delta V/\partial t$ will be neglected from herein.

The transport equation (1) can be compactly expressed with a generalized potential $\tilde{\mathbf{V}}$, generalized flux $\tilde{\mathbf{I}}$, and generalized conductance $\mathbb{G}$,

$$\tilde{\mathbf{I}} = \mathbb{G}\tilde{\mathbf{V}},$$
$$\begin{bmatrix} I_e(f) \\ I_Q(f) \end{bmatrix} = \begin{bmatrix} L'_{11} & L'_{12} \\ L'_{21} & L'_{22} + i2\pi f T C'_Q \end{bmatrix} \begin{bmatrix} \Delta V(f) \\ \Delta T(f)/T \end{bmatrix}, \tag{3}$$

where the Fourier transform $x(f) = \int e^{2\pi i f t} x(t) \mathrm{d}t$ is used to work in the frequency domain, and the limit of frequency below electrical cut-off, $f \ll f_e$ is considered.

The fluctuation-dissipation theorem applied to the generalized potential $\tilde{\mathbf{V}}$ gives

$$S_{\alpha,\beta} = 4k_B T \mathrm{Re}\left[\mathbb{G}^{-1}_{\alpha,\beta}\right], \tag{4}$$

where the spectral density of fluctuations $S_{\alpha,\beta}(f)$ is defined,

$$S_{\alpha,\beta}(f) = \frac{2}{\mathcal{T}}\langle \tilde{\mathbf{V}}_\alpha(+f)\tilde{\mathbf{V}}_\beta(-f)\rangle, \tag{5}$$

where $\langle x \rangle$ denotes the ensemble average of x, and $\mathcal{T} = 1/\Delta f$ is the reciprocal bandwidth. From an experimental perspective, $\mathcal{T}$ is the temporal duration of a measurement [30], while in theoretical analysis $\mathcal{T}$ is the period in the periodic model of a stationary physical system [31]. A field theoretical analysis, presented in the Supplementary Material `Supplementarymaterial.pdf` (SM)[1], arrives at a similar result.

The spectral density $S_T(f) = 2\mathcal{T}^{-1}\langle \Delta T(+f)\Delta T(-f)\rangle$ of the temperature fluctuations across the thermoelectric is

$$S_T(f) = 4k_B T^3 \mathrm{Re}[\mathbb{G}^{-1}_{22}] = 4k_B T^2 \frac{G_T^{-1}}{1 + (f/f_T)^2}, \tag{6}$$

[1]The SM is available, including theoretical analysis of electric field and temperature gradient fluctuations, analysis of voltage fluctuation spectral density in a thermoelectric device, circuit model of a thermoelectric device, voltage fluctuation measurement of a thin film resistor, voltage fluctuation measurement of a $N = 105$ thermoelectric micro-device, numerical model fits of voltage fluctuation and impedance spectra, theoretical heat capacity and thermal conductance estimates, Seebeck coefficient measurements.

where $G_T = \kappa A/L$ is the thermal conductance and $2\pi f_T = G_T/C'_Q$ is the thermal cut-off frequency. The total integrated temperature fluctuation, $\langle(\Delta T)^2\rangle = \int_0^\infty S_T \mathrm{d}f = k_B T^2/C'_Q$, in accordance with the result expected from general considerations of statistical mechanics [14].

The spectral density of the voltage fluctuations $S_V(f) = 2\mathcal{T}^{-1}\langle\Delta V(+f)\Delta V(-f)\rangle$ across the thermoelectric is

$$S_V(f) = 4k_B T \mathrm{Re}[\mathbb{G}_{11}^{-1}] = 4k_B T R_0 + S^2 S_T(f). \quad (7)$$

There are voltage fluctuations of Ohmic origin proportional to the transport coefficient $R_0 = L'^{-1}_{11}$, and voltage fluctuations that originate with temperature fluctuations coupled via the thermoelectric coefficient S. A similar relation for the coupling between temperature gradient and electric field fluctuations is derived in the SM.

Combining the results of eqs. (6), (7), we arrive at the central theoretical result for voltage fluctuations in a thermoelectric,

$$S_V(f) = 4k_B T R_0 \left[1 + \frac{zT}{1+(f/f_T)^2}\right]. \quad (8)$$

In the high-frequency limit above the thermal cut-off frequency, $f \gg f_T$, the usual Johnson-Nyquist formula for spectral density of voltage fluctuations applies, $S_V = 4k_B T R_0$. The spectral density of temperature fluctuations diminish $S_T(f) \propto f^{-2}$ for $f \gg f_T$. In contrast, in the low-frequency limit below thermal cut-off, $f \ll f_T$, there is an enhancement in spectral density of voltage fluctuation beyond the usual Johnson-Nyquist result, $S_V = 4k_B T R_0(1+zT)$. The low-frequency spectral density of temperature fluctuations, $S_T \to 4k_B T^2 G_T^{-1}$, contributes to the observable voltage fluctuations via thermoelectric coupling. The dimensionless zT determines the relative enhancement of voltage noise beyond the Johnson-Nyquist result. Thermoelectric noise enhancement is thus anticipated in materials with large Seebeck coefficient S, large electrical conductivity σ, and small thermal conductivity κ.

Integrated thermoelectric micro-devices. To confirm our theoretical findings, we measured the voltage noise spectral density of integrated, wide-bandwidth, thermoelectric cooling micro-devices. The devices consist of a series network of $L = 10\ \mu$m thick n-type ($Bi_2(Te_{0.95}Se_{0.05})_3$), abbreviated as BiTeSe) and p-type (pure Te) thermoelectric materials, with Au contacts, arranged in serpentine fashion on a Si substrate, as shown in fig. 1(A). A Λ architecture is adopted, fig. 1(B), such that the contra-oriented electrical current I_e in each leg results in co-oriented heat current I_Q in each leg. A microfabricated structure, fig. 1(C) and fig. 1(D), was used to achieve a high thermal cut-off frequency $f_T \sim 1$ kHz, as confirmed by experiment. The cross-sectional areas of the p-type and n-type legs are $A_p = 85\ \mu\text{m} \times 30\ \mu\text{m}$ and $A_n = 30\ \mu\text{m} \times 30\ \mu\text{m}$, respectively. The device systematically studied in our work consisted of 112 series leg pairs. The

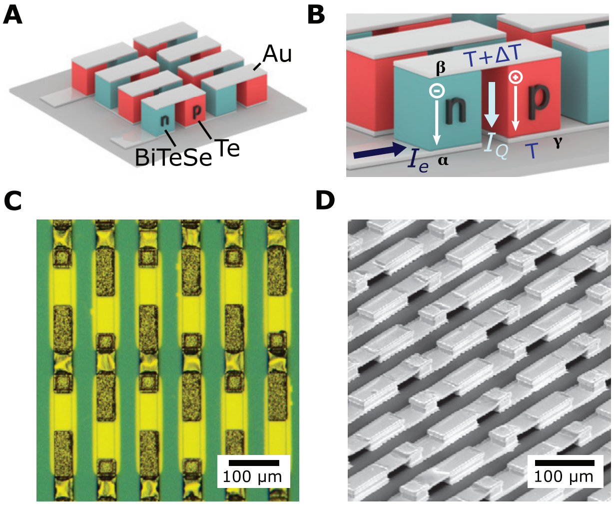

Fig. 1: Integrated thermoelectric cooler. (A) Illustration of the alternating n-type BiTeSe and p-type Te thermoelectric legs with Au electrodes, arranged in a serpentine, series pattern on a substrate. (B) Diagram demonstrating the direction of heat current I_Q downward in both n-type and p-type material as electrical current I_e passes from left to right in the Λ architecture of an n/p pair. (C) Optical microscope image of the fabricated thermoelectric micro-device. (D) Oblique angle scanning electron microscope image of the fabricated thermoelectric micro-device.

spectral density of voltage fluctuations for a thermolectric material in eq. (8) can be extended to a thermoelectric device consisting of a series of N identical leg pairs.

Consider first the voltage fluctuation across a single leg pair in the Λ geometry of fig. 1(B). The points α and γ are fixed at a temperature T determined by the substrate, while the point β is free to fluctuate to a temperature $T + \Delta T$. The fluctuations in temperature difference ΔT across the n-type and p-type legs involve both electrons and phonons and have a spectral density

$$S_T(f) = 4k_B T^2 \frac{(G_n+G_p)^{-1}}{1+(f/f_{T,\Lambda})^2}, \quad (9)$$

where $G_n = \kappa_n A_n/l$, $G_p = \kappa_p A_p/l$ are the thermal conductances of each leg, l is the length of each leg, and the thermal cut-off frequency $2\pi f_{T,\Lambda} = (G_n+G_p)/C'_{Q,\Lambda}$ where $C'_{Q,\Lambda}$ is the total heat capacity for establishing a temperature difference ΔT across the leg pair. The voltage fluctuations across the n-leg $(\alpha-\beta)$ and p-leg $(\beta-\gamma)$ that arise from thermoelectric transduction of temperature fluctuations are correlated, and given by $(S_p - S_n)^2 S_T(f)$. The voltage fluctuations across distinct leg pairs are not correlated, and thus the expected spectral density of voltage fluctuation across the series of N leg pairs in our thermoelectric device is

$$S_V(f) = 4k_B T N(R_n + R_p)\left[1 + \frac{Z_D T}{1+(f/f_{T,\Lambda})^2}\right], \quad (10)$$

where R_i and S_i are the electrical resistance and Seebeck coefficient of the i-type leg, $i = n$, p, and $Z_D T$ is the thermoelectric device figure of merit,

$$Z_D T = \frac{T(S_p - S_n)^2}{(R_n + R_p)(G_n + G_p)}. \quad (11)$$

See the SM for more detail on the derivation of eq. (10).

The voltage fluctuation of the thermoelectric micro-device, eq. (10), differs from the voltage fluctuation of a thermoelectric material, eq. (8), albeit sharing a similar form. Note that the *device* figure of merit $Z_D T$ is not the sum of the constituent *material* figures of merit zT, due to the correlated temperature difference ΔT across p- and n-legs [6].

The origin of the device $Z_D T$ figure of merit in the increase of spectral density of voltage fluctuations can be understood as follows. At frequencies below thermal cut-off, $f \ll f_{T,\pi}$, the spectral density of temperature fluctuations, $S_T = 4k_B T^2 (G_n + G_p)^{-1}$, is inversely proportional to device thermal conductance. The Seebeck effect leads to an additional voltage spectral density $\Delta S_V = (S_p - S_n)^2 S_T$, proportional to the square of device Seebeck coefficient. Since the Ohmic contribution to voltage fluctuations is proportional to the device electrical resistance, $S_{V,\text{Ohmic}} = 4k_B T(R_n + R_p)$, the relative size of the thermoelectric contribution to the Ohmic contribution, $\Delta S_V / S_{V,\text{Ohmic}} = Z_D T$. In other words, $Z_D T$ is the dimensionless parameter that defines the ratio of thermoelectric to Ohmic contributions of voltage fluctuations.

Voltage power spectral density. The spectral density of the voltage across the thermoelectric is reconstructed using a voltage cross correlation method as shown in fig. 2(A). The comparatively high thermal cut-off frequency, $f_{T,\Lambda} \sim 1\,\text{kHz}$, is essential to avoid measurements in the extremely low frequency (ELF, $f < 30\,\text{Hz}$) band where amplifier $1/f$ noise is prohibitively large. Frequency-independent measurement system response over the bandwidth $200\,\text{Hz} < f < 20\,\text{kHz}$ was confirmed using a resistor of $R = 25.9\ \Omega$ (see the SM). The gain in the noise measurement system was calibrated with an $R = 8.20\ \Omega$ resistor at $f = 1.7\,\text{kHz}$.

The measured voltage spectral density $S_V(f)$ *vs.* frequency f is shown in fig. 2(B), along with a numerical fit to eq. (10). Measurements were taken with the thermoelectric substrate temperature T varied from 295 K to 365 K, adjusted with an external resistive heater and measured via thermistor. The dashed horizontal lines denote the Ohmic Johnson-Nyquist noise contribution, $4k_B TN(R_n + R_p)$, with the resistance $N(R_n + R_p)$ determined from the fit of the measured S_V to eq. (10). There is an enhancement in voltage fluctuations $\Delta S_V = S_V - 4k_B TN(R_n + R_p)$ in the low-frequency limit $f \ll f_T$ as compared to the high-frequency limit $f \gg f_T$, indicated with vertical arrows. The increase in low-frequency voltage fluctuations cannot be accounted for by $1/f$ noise, which has a much stronger frequency dependence than that experimentally observed here. Moreover, the model fit permits extraction of various physical parameters such as the heat capacity of a leg-pair, $C'_{Q,\Lambda} = 55.2\,\text{nJ/K}$ at 295 K, which is in good agreement with the theoretically predicted value of 52.4 nJ/K (see the SM).

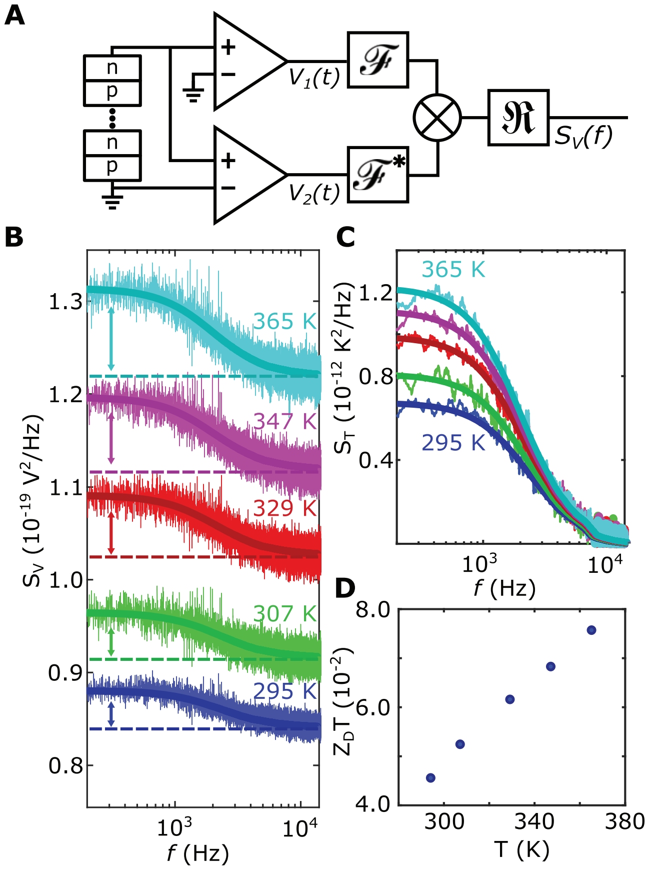

Fig. 2: Voltage and temperature fluctuations. (A) Circuit diagram of the cross-periodogram method used to estimate the spectral density $S_V(f)$ of voltage fluctuations across the thermoelectric micro-device. Independent measurements $V_1(t)$ and $V_2(t)$ are acquired and digitally Fourier transformed to reconstruct S_V from the cross-spectral density. (B) Voltage spectral density $S_V(f)$ *vs.* frequency f of the thermoelectric micro-device measured at a substrate temperature T from 295 K to 365 K. Solid dark lines show a fit to theoretical spectral density of eq. (10). The Ohmic Johnson-Nyquist contributions $4k_B TN(R_n + R_p)$ are indicated with dashed lines, and the excess spectral density $\Delta S_V = S_V - 4k_B TN(R_n + R_p)$ arising from thermoelectric coupling is indicated with vertical arrows. (C) The temperature fluctuation spectral density $S_T(f) = \Delta S_V / S^2$ *vs.* frequency f, using the independently measured, temperature-dependent, effective Seebeck coefficient S. A 40 Hz running average was applied to S_T for visual clarity, and a model fit to eq. (9) is shown. (D) The thermoelectric micro-device figure of merit $Z_D T = \lim_{f \to 0} \Delta S_V / (S_V - \Delta S_V)$ *vs.* substrate temperature T.

Temperature power spectral density. The spectral density of temperature fluctuations, $S_T = \Delta S_V / S^2$, was determined using the effective, temperature-dependent, Seebeck coefficient $S = S_p - S_n$. The Seebeck coefficients of BiTeSe and Te were measured *vs.* temperature (see the SM). For example, at $T = 298\,\mathrm{K}$, $S_p = 194\,\mu\mathrm{V\,K^{-1}}$, $S_n = -44\,\mu\mathrm{V\,K^{-1}}$ and $S = 238\,\mu\mathrm{V\,K^{-1}}$. The experimentally determined spectral density of temperature fluctuations, S_T, is shown in fig. 2(C) *vs.* substrate temperature T, along with a model fit to eq. (9). At $T = 295\,\mathrm{K}$, the experimentally resolved amplitude of temperature fluctuations is $\delta T = S_T^{1/2} = 0.8\,\mu\mathrm{K Hz^{-1/2}}$, corresponding to a relative fluctuation amplitude $\delta T/T = 3 \times 10^{-9}\,\mathrm{Hz^{-1/2}}$. We have thus demonstrated that the remarkably small size of temperature fluctuations in our micro-device can be measured using the Seebeck effect. In the general context of thermometry, our findings show that a thermoelectric micro-device can be used to measure temperature differences as small as the fundamental fluctuations described by the fluctuation-dissipation theorem.

The micro-device figure of merit $Z_D T$ can be determined from the frequency-dependent voltage noise S_V, with $Z_D T = \lim_{f\to 0} \Delta S_V/(S_V - \Delta S_V)$. The figure of merit $Z_D T$ *vs.* substrate temperature T is shown in fig. 2(D), where $Z_D T$ was determined from a fit of the experimentally measured S_V to eq. (10). As anticipated, $Z_D T$ increases with substrate temperature T.

Impedance spectroscopy. The fluctuation-dissipation theorem identifies the equivalency of the coefficient for fluctuation at thermal equilibrium and the coefficient for dissipative transport. We therefore investigated this equivalency for thermoelectrics. The transport equation (1) leads to a frequency-dependent electrical impedance,

$$Z(f) = \frac{\Delta V}{I_e} = R\left(1 + \frac{Z_D T}{1 + if/f_{T,\Lambda}}\right), \qquad (12)$$

where $R = N(R_n + R_p)$ for our thermoelectric micro-device. The impedance of eq. (12) is the basis for impedance spectroscopy of thermoelectrics, which have evolved in complexity [32–36]. The Nyquist plot of measured $-\mathrm{Im}\{Z\}$ *vs.* $\mathrm{Re}\{Z\}$ is shown in fig. 3(A) at $T = 295\,\mathrm{K}$, 329 K, and 365 K. The semi-circle characteristic of first-order response is evident in the Nyquist plot, and a numerical fit to the simple model of eq. (12).

Discussion. – A direct comparison of the measured dissipative impedance coefficient $\mathrm{Re}\{Z\}$ and the measured normalized voltage fluctuation spectral density $S_V/4k_BT$ is shown in fig. 3(B). Our experiments are in good agreement with the fluctuation-dissipation theorem as applied to the effective electronic sector of the transport equations, $\mathrm{Re}\{Z\} = S_V/4k_BT$. The thermoelectric coupling thus simultaneously enhances both the spectral density of voltage fluctuations and the electrical impedance above that of the purely Ohmic contribution to each. Voltage fluctuations are enhanced by thermoelectric coupling of temperature fluctuations. Impedance is enhanced by the voltage generated by thermoelectric coupling to the temperature gradient established by the passage of electrical (and thus heat) current in the thermoelectric.

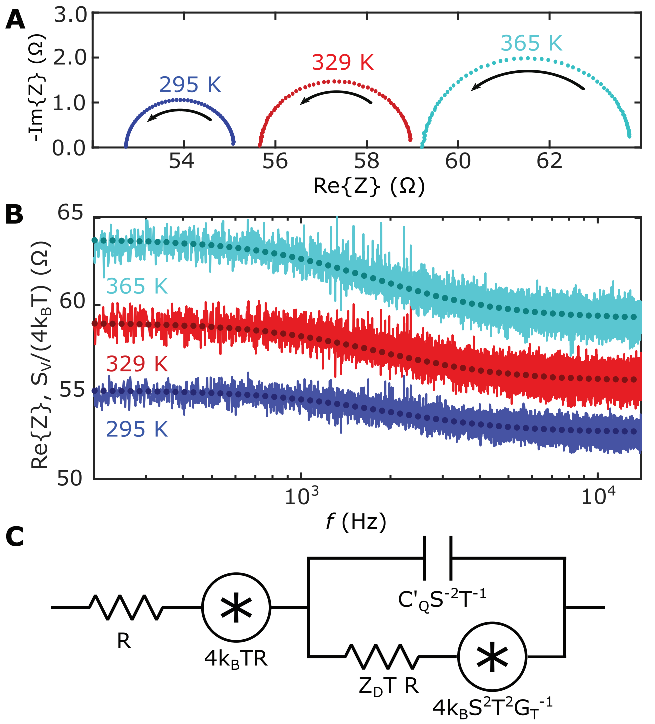

Fig. 3: Impedance and noise spectroscopy. (A) Nyquist plot of the measured impedance, $-\mathrm{Im}\{Z\}$ *vs.* $\mathrm{Re}\{Z\}$ at $T = 295\,\mathrm{K}$, 329 K, and 365 K, over the frequency $100\,\mathrm{Hz} < f < 100\,\mathrm{kHz}$. The semi-circle arrow direction indicates an increase in frequency. (B) A comparison of the measured dissipative impedance $\mathrm{Re}\{Z\}$ (dark circles) and the measured voltage spectral density normalized to impedance units, $S_V/4k_BT$, (coloured lines) *vs.* frequency f. (C) Model circuit for a thermoelectric, including Ohmic and thermoelectric dissipative elements, Ohmic and thermolectric fluctuation sources, and effective capacitance.

Assembling our findings, a simple equivalent electrical transport model for a thermoelectric element is shown in fig. 3(C), using simplified notation (see the SM for further detail). The model includes the Ohmic resistance R and associated Johnson-Nyquist fluctuations of spectral density $4k_BTR$, a resistance $Z_DT \cdot R = TS^2G_T^{-1}$ of thermoelectric origin with an associated spectral density of voltage fluctuations $4k_BTR \cdot Z_DT = 4k_BS^2T^2G_T^{-1}$. The frequency dependence of thermal contributions to impedance and voltage fluctuations is accounted for with the inclusion of an effective capacitance $C_T = C'_Q T^{-1} S^{-2}$ of thermal origin, with cut-off frequency $2\pi f_T = G_T/C_T$.

Our model is readily extended to a variety of other contexts involving thermoelectrics. Changes to the thermal environment can be incorporated by modifying the thermal circuit. For example, loading the top conductor of a Λ leg-pair introduces an additional heat capacity and a thermal conductance to the environment. The effect of increasing heat capacity is to reduce the thermal cut-off frequency. The effect of increased thermal conductance is to reduce the effective Z_DT, but care must be taken to account for time-dependent heat diffusion through the thermal load, as observed by impedance spectroscopy of thermoelectric devices [34–36]. By the general arguments presented in this work, the power spectral density of voltage fluctuations will be modified by thermal loading in analogous fashion to the modification of the dissipative component of impedance. Finally, we note that our model can be easily extended to include the electrical environment of a thermoelectric device, including capacitive and inductive effects.

Conclusions. – In conclusion, we have demonstrated how the fluctuation-dissipation theorem can be extended to thermoelectrics, revealing the role of temperature fluctuations in the modification of the renowned Johnson-Nyquist formula. Our work establishes a quantitative model for the temperature fluctuations and voltage fluctuations inherent to a thermoelectric device as a consequence of the fluctuation-dissipation theorem. The temperature fluctuation $\delta T = S_T^{1/2}$ defines an important physical limit to temperature measurement by microscale thermoelectric thermometry, and is expected to be of importance to applications such as intracellular thermometry [23]. Finally, we note that our results can be generalized to include other physical quantities carried by fundamental excitations in a conductor. For example, spin-orbit coupling can result in fundamental excitations that carry charge and spin, and the correlated transport of charge and spin can in principle lead to a modification of the observable spectral density of voltage fluctuations. Moreover, the spectral density of voltage fluctuations may give insight into the spectral density of spin fluctuations.

Materials and methods. – The thermoelectric micro-coolers were fabricated using standard photolithography and a modified electrochemical deposition technique, details can be found in [29]. The voltage power spectral density $S_V(f)$ was measured using a correlation method, as shown in fig. 2(A). The voltage across two terminals of a series of p/n leg pairs was measured simultaneously with two cascaded voltage amplifiers. Each cascade consisted of two identical voltage pre-amplifiers (LI-75, NF Corp.) with 40 dB total gain. The voltages $V_1(t)$ and $V_2(t)$ were digitized (DT-9847, Data Translation) and the cross-spectral density estimated using the cross-periodogram method [30]. To suppress the uncorrelated amplifier noise in $V_1(t)$ and $V_2(t)$, we averaged 7.5×10^4 periodograms, with 2.15×10^5 samples/periodogram acquired at a sampling rate of 2.15×10^5 samples/s, for over 20hours of acquisition time per spectral density measurement. The micro-device was placed in a series of metal boxes for electrical and thermal isolation, open-loop resistive heating was applied to vary the sample substrate temperature T, and a thermistor was used to measure the mean temperature T, which varied by less than ± 1 K over the duration of each measurement.

The Seebeck coefficient of both the n-type and p-type thermoelectric legs was inferred from measurements of BiTeSe and Te thin films, with further details provided in the SM. The thermoelectric device impedance was measured using a lock-in amplifier (MLFI 500 kHz, Zurich Instruments) with an AC current bias I_e of 100 μA amplitude over a frequency range 100 Hz $< f <$ 100 kHz.

* * *

A-MST, BR and TS acknowledge financial support from the Natural Sciences and Engineering Research Council of Canada (NSERC) under grants RGPIN-2016-04400, RGPIN-2018-04851, RGPIN-2019-05312, the Canada First Research Excellence Fund, and the Canada Excellence Research Chairs program. ASD, HR and GS acknowledge funding from the DFG (Deutsche Forschungsgemeinschaft) under grant No. SCHI1010/11-1, and NBP and HR acknowledge funding under grant No. RE3973/1-1. ASD, NBP, HR, KN and GS fabricated the integrated thermoelectric micro-device and measured the Seebeck coefficient of the n-type and p-type thermoelectric material. The theoretical derivations were done by NAMT, AMST, BR, and TS. NAMT acquired all the noise measurements with the assistance from AH and AD. The impedance spectroscopy was done by NAMT. NAMT and TS prepared the manuscript with contributions from all co-authors. We have no competing interest to declare.

Data availability statement: The data that support the findings of this study are available upon reasonable request from the authors.

REFERENCES

[1] Callen H. B. and Welton T. A., *Phys. Rev.*, **83** (1951) 34.
[2] Johnson J. B., *Phys. Rev.*, **32** (1928) 97.
[3] Nyquist H., *Phys. Rev.*, **32** (1928) 110.
[4] Gardiner C. and Zoller P., *Quantum Noise* (Springer, New York) 2004.
[5] Ashcroft N. W. and Mermin N. D., *Solid State Physics*, Vol. **2005** (Holt, Rinehart and Winston, New York) 1976.
[6] Rowe D. M., *CRC Handbook of Thermoelectrics* (CRC Press, Boca Raton) 1995.
[7] Goupil C., Seifert W., Zabrocki K., Müller E. and Snyder G. J., *Entropy*, **13** (2011) 1481.
[8] Crépieux A. and Michelini F., *J. Phys.: Condens. Matter*, **27** (2014) 015302.
[9] Dashti N., Misiorny M., Samuelsson P. and Splettstoesser J., *Phys. Rev. Appl.*, **10** (2018) 024007.
[10] Karimi B., Brange F., Samuelson P. and Pekola J. P., *Nat. Commun.*, **11** (2020) 1.
[11] Crépieux A., *Phys. Rev. B*, **103** (2021) 045427.

[12] Marchegiani G., Braggio A. and Giazotto F., *Appl. Phys. Lett.*, **117** (2020) 212601.

[13] Marchegiani G., Braggio A. and Giazotto F., *Phys. Rev. Lett.*, **124** (2020) 106801.

[14] Landau L. D. and Lifshitz E. M., *Course of Theoretical Physics: Statistical Physics Part I* (Elsevier) 1981.

[15] Puglisi A., Sarracino A. and Vulpiani A., *Phys. Rep.*, **709** (2017) 1.

[16] Chui T., Swanson D., Adriaans M., Nissen J. and Lipa J., *Phys. Rev. Lett.*, **69** (1992) 3005.

[17] Richards P., *J. Appl. Phys.*, **76** (1994) 1.

[18] Spahr K., Graveline J., Lupien C., Aprili M. and Reulet B., *Phys. Rev. B*, **102** (2020) 100504.

[19] Nagaev K., *Phys. Rev. B*, **66** (2002) 075334.

[20] Pinsolle E., Houle S., Lupien C. and Reulet B., *Phys. Rev. Lett.*, **121** (2018) 027702.

[21] Zhang Y., Zhu W., Hui F., Lanza M. Borca-Tasciuc T. and Muñoz Rojo, *Adv. Funct. Mater.*, **30** (2020) 1900892.

[22] Shrestha R., Choi T. -Y., Chang W. and Kim D., *Sensors*, **11** (2011) 8826.

[23] Tian W., Wang C., Wang J., Chen Q., Sun J., Li C., Wang X. and Gu N., *Nanotechnology*, **26** (2015) 355501.

[24] Bai T. and Gu N., *Small*, **12** (2016) 4590.

[25] Rajagopal M. C., Valavala K. V., Gelda D., Ma J. and Sinha S., *Sens. Actuators A: Phys.*, **272** (2018) 253.

[26] Harzheim A., Könemann F., Gotsmann B., van der Zant H. and Gehring P., *Adv. Funct. Mater.*, **30** (2020) 2000574.

[27] Zhu P., Wang Y., Wang Y., Mao H., Zhang Q. and Deng Y., *Adv. Energy Mater.*, **10** (2020) 2001945.

[28] Tian B., Liu Z., Wang C., Liu Y., Zhang Z., Lin Q. and Jiang Z., *Rev. Sci. Instrum.*, **91** (2020) 045004.

[29] Li G., Fernandez J. G., Ramos D. A. L., Barati V., Pérez N., Soldatov I., Reith H., Schierning G. and Nielsch K., *Nat. Electron.*, **1** (2018) 555.

[30] Priestley M. B., *Spectral Analysis and Time Series: Probability and Mathematical Statistics* (Academic Press, San Diego) 1981.

[31] Pathria R. K., *Statistical Mechanics* (Butterworth-Heineman, Oxford) 1996.

[32] Harman T. C., *J. Appl. Phys.*, **29** (1958) 1373.

[33] Downey A. D., Hogan T. P. and Cook B., *Rev. Sci. Instrum.*, **78** (2007) 093904.

[34] García-Cañadas J. and Min G., *J. Appl. Phys.*, **116** (2014) 174510.

[35] García-Cañadas J. and Min G., *AIP Adv.*, **6** (2016) 035008.

[36] Hasegawa Y., Homma R. and Ohtsuka M., *J. Electron. Mater.*, **45** (2016) 1886.